

# First measurement of the circular beam asymmetry in the $\vec{\gamma}p \rightarrow \pi^0\eta p$ reaction

V. L. Kashevarov<sup>a,b,\*</sup>, A. Fix<sup>c</sup>, P. Aguar-Bartolomé<sup>a</sup>, L. K. Akasoy<sup>a</sup>,  
 J. R. M. Annand<sup>d</sup>, H. J. Arends<sup>a</sup>, K. Bantawa<sup>e</sup>, R. Beck<sup>f</sup>, V. Bekrenev<sup>g</sup>,  
 H. Berghäuser<sup>h</sup>, A. Braghieri<sup>i</sup>, D. Branford<sup>j</sup>, W. J. Briscoe<sup>k</sup>, J. Brudvik<sup>l</sup>,  
 S. Cherepnya<sup>b</sup>, R. F. B. Codling<sup>d</sup>, B. T. Demissie<sup>k</sup>, E. J. Downie<sup>a,d</sup>,  
 P. Drexler<sup>h</sup>, L. V. Fil'kov<sup>b</sup>, D. I. Glazier<sup>j</sup>, R. Gregor<sup>h</sup>, D. Hamilton<sup>d</sup>,  
 E. Heid<sup>a,k</sup>, D. Hornidge<sup>m</sup>, I. Jaegle<sup>n</sup>, O. Jahn<sup>a</sup>, T. C. Jude<sup>j</sup>, J. D. Kellie<sup>d</sup>,  
 I. Keshelashvili<sup>n</sup>, R. Kondratiev<sup>o</sup>, M. Korolija<sup>p</sup>, M. Kotulla<sup>h</sup>,  
 A. Koulbardis<sup>g</sup>, S. Kruglov<sup>g</sup>, B. Krusche<sup>n</sup>, V. Lisin<sup>o</sup>, K. Livingston<sup>d</sup>,  
 I. J. D. MacGregor<sup>d</sup>, Y. Maghrbi<sup>n</sup>, D. M. Manley<sup>e</sup>, M. Martinez-Fabregate<sup>a</sup>,  
 J. C. McGeorge<sup>d</sup>, E. F. McNicoll<sup>d</sup>, D. Mekterovic<sup>p</sup>, V. Metag<sup>h</sup>,  
 S. Micanovic<sup>p</sup>, D. Middleton<sup>m</sup>, A. Mushkarenkov<sup>i</sup>, B. M. K. Nefkens<sup>l</sup>,  
 A. Nikolaev<sup>f</sup>, R. Novotny<sup>h</sup>, M. Ostrick<sup>a</sup>, P. B. Otte<sup>a</sup>, B. Oussena<sup>a,k</sup>,  
 P. Pedroni<sup>i</sup>, F. Pheron<sup>n</sup>, A. Polonski<sup>o</sup>, S. N. Prakhov<sup>l</sup>, J. Robinson<sup>d</sup>,  
 G. Rosner<sup>d</sup>, T. Rostomyan<sup>n</sup>, S. Schumann<sup>a</sup>, M. H. Sikora<sup>j</sup>, D. Sober<sup>q</sup>,  
 A. Starostin<sup>l</sup>, I. I. Stakovsky<sup>k</sup>, I. M. Suarez<sup>l</sup>, I. Supek<sup>p</sup>, C. Tarbert<sup>j</sup>,  
 M. Thiel<sup>h</sup>, A. Thomas<sup>a</sup>, M. Unverzagt<sup>a</sup>, D. P. Watts<sup>j</sup>, D. Werthmüller<sup>n</sup>,  
 I. Zamboni<sup>p</sup>, and F. Zehr<sup>n</sup>,  
 (The Crystal Ball at MAMI, TAPS, and A2 Collaborations)

<sup>a</sup>*Institut für Kernphysik, Johannes Gutenberg-Universität Mainz, Mainz, Germany*

<sup>b</sup>*Lebedev Physical Institute, Moscow, Russia*

<sup>c</sup>*Tomsk Polytechnic University, Tomsk, Russia*

<sup>d</sup>*Department of Physics and Astronomy, University of Glasgow, Glasgow, UK*

<sup>e</sup>*Kent State University, Kent, OH, USA*

<sup>f</sup>*Helmholtz-Institut für Strahlen- und Kernphysik, Universität Bonn, Bonn, Germany*

<sup>g</sup>*Petersburg Nuclear Physics Institute, Gatchina, Russia*

<sup>h</sup>*II. Physikalisches Institut, Universität Giessen, Giessen, Germany*

<sup>i</sup>*INFN Sezione di Pavia, Pavia, Italy*

<sup>j</sup>*School of Physics, University of Edinburgh, Edinburgh, UK*

<sup>k</sup>*The George Washington University, Washington, DC, USA*

<sup>l</sup>*University of California at Los Angeles, Los Angeles, CA, USA*

<sup>m</sup>*Mount Allison University, Sackville, NB, Canada*

<sup>n</sup>*Institut für Physik, Universität Basel, Basel, Switzerland*

---

\*Corresponding author

Email address: kashev@kph.uni-mainz.de (V. L. Kashevarov)

*<sup>o</sup>Institute for Nuclear Research, Moscow, Russia*  
*<sup>p</sup>Rudjer Boskovic Institute, Zagreb, Croatia*  
*<sup>a</sup>The Catholic University of America, Washington, DC, USA*

---

## Abstract

The circular photon asymmetry for  $\pi^0\eta$  photoproduction on the proton was measured for the first time at the tagged photon facility of the MAMI C accelerator using the Crystal Ball/TAPS photon spectrometer. The experimental results are interpreted within a phenomenological isobar model that confirms the dominant role of the  $\Delta(1700)D_{33}$  resonance. The measured asymmetry allows us to identify small contributions from positive-parity resonances via interference terms with the dominant  $D_{33}$  amplitude.

*Keywords:* Pseudoscalar meson photoproduction, Baryon resonances, Polarization observables

---

The full understanding of the structure and excitation spectrum of the nucleon remains one of the most challenging topics of particle physics. Traditionally, a large amount of information on baryon resonances was provided by scattering or photoproduction of pions. However, despite manifest progress, our knowledge of the properties of many resonances is still rather limited, to the extent that the very existence of some so-called established states [1] is called into question. The production of meson pairs like  $\pi\pi$  or  $\eta\pi$  is an attractive tool to study resonances that couple strongly to intermediate  $\Delta\pi$ ,  $\Delta\eta$  or  $N^*\pi$  states.

In recent years, the empirical information available on the  $\gamma p \rightarrow \pi^0\eta p$  reaction has considerably improved. New data were obtained on the total and differential cross sections as well as on linear beam asymmetries [2, 3, 4, 5, 6, 7]. The observed rapid rise of the total cross section from threshold together with an almost isotropic  $\eta$  angular distribution already indicates that the  $\eta$  meson is mostly emitted into an  $s$ -wave state with respect to the  $\pi^0 p$  system. Considering that the  $\pi^0 p$  interaction is mainly due to excitation of the  $\Delta(1232)$ , this points to the importance of a partial-wave amplitude with spin-parity  $J^P = 3/2^-$  and isospin  $I = 3/2$ . In  $\pi N$  scattering these quantum numbers require a  $d$ -wave and the amplitude is therefore called  $D_{33}$ . It is populated by the  $\Delta(1700)D_{33}$  resonance in the energy region close to the

threshold of the  $\gamma p \rightarrow \pi^0 \eta p$  reaction. Furthermore, within phenomenological models [2, 8, 9, 10] a reasonable description of the total and differential cross sections as well as the measured beam asymmetries [5, 7] can be achieved assuming the dominance of this amplitude. However, the reliable extraction of resonance parameters and the study of small contributions from other partial-wave amplitudes require measuring additional spin observables. The nontrivial role of such resonances was indicated by the PWA analysis of ref. [2] as well as by measurements of the angular distributions presented in refs. [6, 9].

The general structure of the cross section for the photoproduction of two pseudoscalar mesons and the definition of spin observables is discussed in ref. [11]. The circular beam asymmetry  $I^\odot$  has been measured in double pion photoproduction [12, 13]. In the case of  $\pi\eta$  photoproduction related observables,  $I^s$  and  $I^c$ , have recently been measured with a linearly polarized beam [14]. Model calculations [15, 16] clearly demonstrate the strong sensitivity of these spin observables to the dynamical content of the reaction amplitude.

In this Letter we present first measurements of the circular beam asymmetry in the reaction  $\vec{\gamma}p \rightarrow \pi^0 \eta p$ . The experiment was performed with the Crystal Ball/TAPS hermetic spectrometer system at the Glasgow tagged photon facility [17] of the MAMI C accelerator in Mainz [18]. The experimental setup and the event selection procedure are described in detail in [6]. The data were taken in April 2009 (300 hours with a 10 cm long liquid hydrogen target and a beam current of 10 nA).

The usual circular photon asymmetry (in the literature also called the helicity photon asymmetry) is defined as

$$I^\odot(\phi) = \frac{1}{P_\gamma} \frac{d\sigma^+ - d\sigma^-}{d\sigma^+ + d\sigma^-}, \quad (1)$$

where  $d\sigma^+(d\sigma^-)$  denote the 5-fold differential cross sections integrated over the energy of the  $\eta$  meson, its solid angle,  $d\Omega_\eta$ , and the polar angle of the pion,  $d\Theta_\pi$ , for beam helicities  $\lambda_\gamma = \pm 1$ .  $P_\gamma$  is the degree of circular beam polarization. The argument  $\phi$  is the angle between the reaction plane and the plane spanned by the momenta of the produced pion and the proton in the final state (see Fig. 1). It is equal to the pion azimuthal angle in the  $\pi N$  c.m. frame with the  $z$ -axis being in the opposite direction to the  $\eta$  momentum. In the case of a two-body final state, the asymmetry  $I^\odot$  vanishes exactly.

In what follows, we will consider an observable whose definition slightly

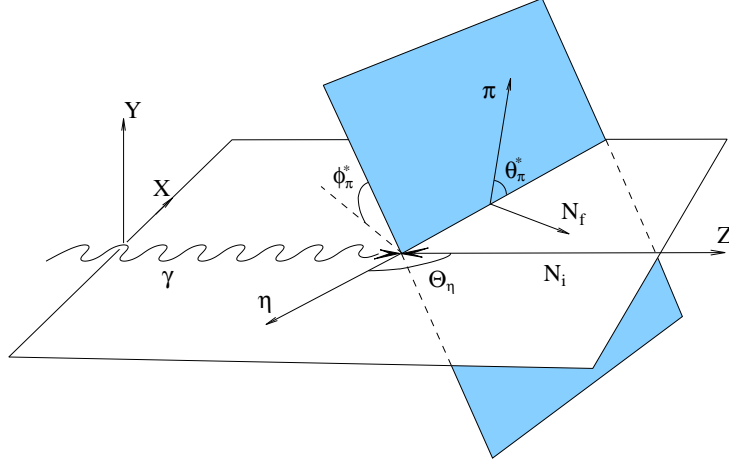


Figure 1: Diagrams representing the angles  $\Theta_\eta$  and  $\Omega = (\theta, \phi)$  used for description of the reaction kinematics.

differs from (1), namely

$$W^c(\phi) = \frac{2\pi}{\sigma} I^\odot(\phi) \frac{d\sigma}{d\phi} = \frac{1}{P_\gamma} \frac{\pi}{\sigma} \frac{d\sigma^+ - d\sigma^-}{d\phi}, \quad (2)$$

where the unpolarized cross section is defined as

$$\frac{d\sigma}{d\phi} = \frac{1}{2} \frac{d\sigma^+ + d\sigma^-}{d\phi} \quad (3)$$

and  $\sigma$  stands for the integrated (total) cross section,

$$\sigma = \int_0^{2\pi} \frac{d\sigma}{d\phi} d\phi. \quad (4)$$

As can readily be seen from (1) and (2), the only difference between the quantity  $W^c$  and the asymmetry  $I^\odot$  is that the former contains in the denominator not the differential cross section at a given angle  $\phi$  but its average over the whole  $\phi$  region, which is equal to the total cross section  $\sigma$  divided by  $2\pi$ . Contrary to  $I^\odot$ , the function  $W^c$  does not contain any  $\phi$ -dependence in the denominator, thus the most interesting part, the angular dependence of the helicity difference  $d\sigma^+ - d\sigma^-$ , is directly visible.

The asymmetry  $W^c$  is determined from the experimental data, using the number of reconstructed events for each helicity corrected for the detector

acceptance and photon flux. All other normalization factors cancel in the ratio (2). The degree of polarization,  $P_\gamma$ , is given by the electron beam polarization multiplied by a well known factor describing the helicity transfer to photons in bremsstrahlung processes [19] which varies between 84% and 99% in our photon energy range. The electron beam polarization was measured by Mott and Moeller scattering to be  $P_e = (80.9 \pm 2.5)\%$ .

The results for the observable  $W^c$  are shown in Fig. 2 for different beam energy bins with statistical uncertainties only. The systematic uncertainty is dominated by the contribution from the beam polarization. Further contributions from acceptance calculations and flux normalization are negligible.

Due to parity conservation the cross sections for different photon helicities are related by

$$d\sigma^+(-\phi) = d\sigma^-(\phi). \quad (5)$$

Then the relations

$$W^c(2\pi - \phi) = W^c(-\phi) = -W^c(\phi) \quad (6)$$

immediately follow from the definition in eq.(2). As a consequence,  $W^c(\phi)$  may be Fourier-expanded over the functions  $\sin n\phi$ ,

$$W^c(\phi) = \sum_{n=1}^{n_{\max}} A_n \sin n\phi. \quad (7)$$

In the absence of a strong background, the maximum value of  $n$  is determined by the maximum spin of the contributing resonances. The same features were demonstrated for  $2\pi$  photoproduction in refs. [12, 13]. While in the channels with charged pions ( $\pi^+\pi^-$ ,  $\pi^0\pi^+$ ) the asymmetry  $I^\odot(\phi)$  exhibits quite a complicated angular dependence, due to strong background contributions, the  $\pi^0\pi^0$  production is easily fitted by  $\sin 2\phi$ . As in  $\pi^0\eta$ , the production of two neutral pions is dominated by resonance excitations, whereas, in the charge channels, different peripheral background mechanisms become important. These are responsible for the rather complex angular dependence of the helicity asymmetry.

To fit our data for  $W^c(\phi)$  we retain the first three terms in eq. (7). The results are presented in Fig. 2 by the dotted line. In Fig. 3 the first three coefficients  $A_1$ ,  $A_2$ , and  $A_3$  from the series (7) are plotted as functions of the photon energy. The first term in the series is most important. The terms with  $n = 2$  and  $n = 3$  are significantly suppressed.

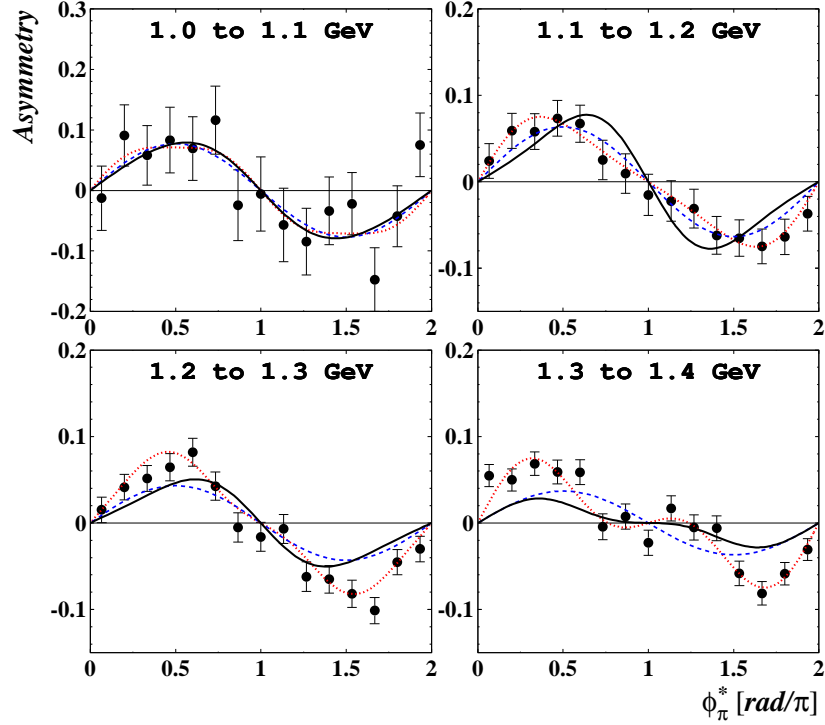


Figure 2: Angular distributions of the cross-section asymmetry  $W^c(\phi)$  for the reaction  $\bar{\gamma}p \rightarrow \pi^0\eta p$  as determined according to eq. (2). The dotted curve is our fit with three terms included in the Fourier expansion (7). The solid curves show predictions of the full isobar model with six resonances whose parameters were fitted to the angular distributions for  $\gamma p \rightarrow \pi^0\eta p$  as described in ref. [9]. The dashed curve is a similar prediction with only the  $D_{33}$  amplitude taken into account.

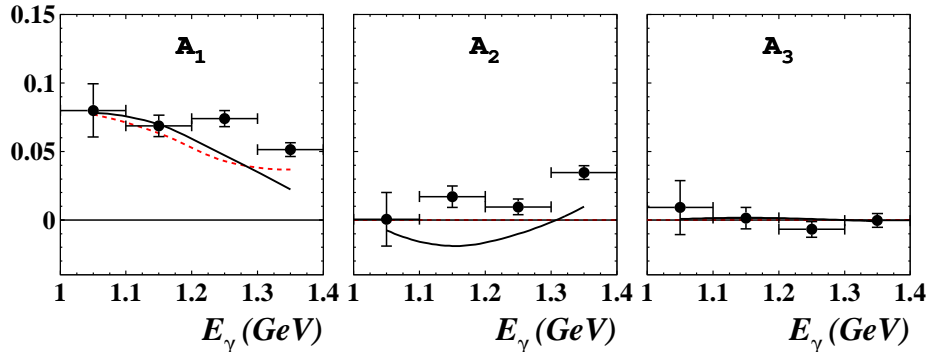


Figure 3: Coefficients  $A_n$  ( $n = 1, 2, 3$ ) of the  $\sin n\phi$  expansion of the asymmetry  $W^c(\phi)$ , Eq. (7). The solid line is the full model prediction, the dashed line includes only the  $D_{33}$  amplitude.

In the same figure we show model predictions obtained with the formalism developed in refs. [9] and all parameters fixed by fitting the angular distributions with only a  $D_{33}$  amplitude (dashed) and the full isobar model (solid). Here we limit ourselves to a brief overview of the formal basis. The general structure of the matrix element is represented by a background amplitude  $t_{m_f\lambda}^B$  and a resonance part  $t_{m_f\lambda}^R$ :

$$t_{m_f\lambda} = t_{m_f\lambda}^B + \sum_{R(J^\pi;T)} t_{m_f\lambda}^R, \quad (8)$$

where the summation is over the resonance states  $R(J^\pi;T)$  determined by their spin-parity  $J^\pi$  and the isospin  $T$ . The indices  $m_f = \pm 1/2$  and  $\lambda = \pm 1/2, \pm 3/2$  denote respectively the  $z$ -projection of the final nucleon spin and the initial state helicity.

In the isobar model the transition to the three particle state  $\pi\eta N$  is described in terms of intermediate decays into the  $\eta + P_{33}(1232)$  and  $\pi + S_{11}(1535)$  states, followed by the decay of the  $P_{33}(S_{11})$  resonance into  $\pi N(\eta N)$ . The resonance amplitudes are accordingly decomposed into two parts

$$t_{m_f\lambda}^R = t_{m_f\lambda}^{R(\eta\Delta)} + t_{m_f\lambda}^{R(\pi N^*)}, \quad (9)$$

where we use the notations  $\Delta$  and  $N^*$  for  $P_{33}(1232)$  and  $S_{11}(1535)$ , respectively.

The polarized cross section is expressed as a difference between quadratic forms of the amplitudes (8) with different helicities:

$$I^\odot \frac{d\sigma}{d\phi} \sim \sum_{m_f, \lambda=\frac{1}{2}, \frac{3}{2}} \int \left( |t_{m_f\lambda}|^2 - |t_{m_f-\lambda}|^2 \right) d\text{Ps}, \quad (10)$$

$d\text{Ps}$  is the appropriate element of the phase space.

As is shown in [9, 10] the background is small, so that we neglect its contribution and assume that in our energy region the reaction is dominated by the  $D_{33}$  amplitude accompanied by a relatively small admixture of other partial waves, in our case  $P_{31}$ ,  $P_{33}$ , and  $F_{35}$  which contribute via interference with the dominant  $D_{33}$  excitation. Keeping only interference terms which are linear in the ‘weak’ amplitudes, the integrand in eq. (10) calculated to the first order in  $t^{P_{31}}$ ,  $t^{P_{33}}$ , and  $t^{F_{35}}$  reads

$$\begin{aligned} |t_{m_f\lambda}|^2 - |t_{m_f-\lambda}|^2 \simeq & \left| t_{m_f\lambda}^{D_{33}} \right|^2 + 2\Re \left\{ \bar{t}_{m_f\lambda}^{D_{33}} t_{m_f\lambda}^{P_{31}} \right. \\ & \left. + \bar{t}_{m_f\lambda}^{D_{33}} t_{m_f\lambda}^{P_{33}} + \bar{t}_{m_f\lambda}^{D_{33}} t_{m_f\lambda}^{F_{35}} \right\} - (\lambda \rightarrow -\lambda), \end{aligned} \quad (11)$$

where  $\bar{t}$  means the complex conjugated value. Using eq. (11) one obtains for the asymmetry (2) the following expression [20]:

$$W^c(\phi) = A_1 \sin \phi + A_2 \sin 2\phi. \quad (12)$$

Explicit expressions for the coefficients  $A_n$  are not important for the discussion below. They will be presented in a separate paper [20]. Here we simply summarize the key points to demonstrate the main physical ideas. The first coefficient in eq. (12),  $A_1$ , is determined solely by the  $D_{33}$  wave. Actually, it also contains terms that are quadratic in ‘small’ partial-wave amplitudes. However, as noted above, the latter were neglected here due to their insignificance. It is also worth noting that  $D_{33}$  contributes to the asymmetry  $W^c(\phi)$  only because the decay modes,  $D_{33} \rightarrow \pi N^*$  and  $D_{33} \rightarrow \eta \Delta$ , interfere with each other. In [6] the contribution of the  $D_{33} \rightarrow \pi N^*$  decay was identified using the characteristic form of the pion angular distribution in the  $\pi N$  c.m. system. The present results for  $W^c(\phi)$  are additional independent evidence for the importance of this decay channel.

If only the linear contribution of ‘weak’ resonance amplitudes is retained they enter only the second term of eq. (12). In other words, the  $\sin 2\phi$  admixture in the asymmetry  $W^c$  appears only through the interference of these



states with the dominant  $D_{33}$  wave. It can be shown [20] that the appearance of this term in the expansion (12) is caused by the different parity of the resonances  $P_{31}$ ,  $P_{33}$ , and  $F_{35}$  relative to the dominant  $D_{33}$  state. In this respect, the term with  $\sin 2\phi$  is a signature of positive parity states entering the amplitude.

The solid curves in these figures show predictions of the full isobar model including the  $D_{33}(1700)$ ,  $P_{33}(1600)$ ,  $P_{31}(1750)$ ,  $F_{35}(1905)$ ,  $P_{33}(1920)$ , and the  $D_{33}(1940)$ . The dashed curve includes only the  $D_{33}$  amplitude. The resonance parameters were taken from ref. [9] where they were obtained by fitting the measured angular distributions [6]. We use the parameter set, corresponding to Solution I compiled in Table II of ref. [9] which also provides reasonable agreement with the measured beam asymmetry [5, 14]. The present data were not used in the fit. In view of strong sensitivity of  $W^c$  to the resonance content of the amplitude, in particular to the interference effects between different partial waves, the quality of description in Figs. 2 and 3 is rather good. Nevertheless, systematic deviations at higher energies point to necessity for further improvements of the theory. As one can see, at  $E_\gamma > 1.2$  GeV our calculation underestimates the coefficient  $A_1$ . In this region the single  $D_{33}$  model (only the  $D_{33}$  wave is included) provides even a slightly better description of the asymmetry. The coefficient  $A_2$  is predicted to be negative in contrast to the experimental value, although the general tendency of its behavior, the monotonic increase with the energy, is roughly reproduced. The coefficient  $A_3$ , proportional to squares of the ‘weak’ amplitudes, is comparable with zero in the whole energy region, in accordance with the data.

In summary, we presented first measurements of the circular photon asymmetry in the reaction  $\vec{\gamma}p \rightarrow \pi^0\eta p$ . Our purpose was to explore the contribution of resonances with positive parity, which manifest themselves primarily in polarization observables via interference with the dominating  $D_{33}$  partial wave. The experimental results were compared to the model predictions with the parameters fixed in ref. [9] by fitting the unpolarized angular distributions of ref. [6]. The comparison demonstrates that the single  $D_{33}$  model roughly reproduces the gross features of the observed helicity asymmetry. At the same time, in the region  $E_\gamma > 1.3$  GeV the positive parity resonances start to come into play, resulting in strong increase of the  $\sin 2\phi$  term in the Fourier expansion (7). The full isobar model of ref. [9] including  $P_{33}(1600)$ ,  $P_{31}(1750)$ ,  $F_{35}(1905)$ , and  $P_{33}(1920)$  states demonstrates certain shortcomings, especially at higher energies. The present measurements together with

the linear beam asymmetry presented in ref. [7] open a path for further improvements of the theoretical description of  $\pi^0\eta$  photoproduction.

The authors wish to acknowledge the excellent support of the accelerator group and operators of MAMI. This work was supported by the Deutsche Forschungsgemeinschaft (SFB 443, SFB/TR16), DFG-RFBR (Grant No. 09-02-91330), the European Community-Research Infrastructure Activity under the FP6 “Structuring the European Research Area” programme (Hadron Physics, contract number RII3-CT-2004-506078), Schweizerischer National fonds, the UK Engineering and Physical Sciences Research Council, U.S. DOE, U.S. NSF, and NSERC (Canada). A.F. acknowledges additional support from the RF Federal programm “Kadry”. We thank the undergraduate students of Mount Allison University and The George Washington University for their assistance.

## References

- [1] C. Amsler, et al., [Particle Data Group], Phys. Lett. B 667 (2008) 1.
- [2] I. Horn, et al., [CBELSA collaboration], Eur. Phys. J. A 38 (2008) 173.
- [3] Ch. Weinheimer, et al., Nucl. Phys. A 721 (2003) 781c.
- [4] T. Nakabayashi, et al., Phys. Rev. C 74 (2006) 035202.
- [5] J. Ajaka, et al., Phys. Rev. Lett. 100 (2008) 052003.
- [6] V.L. Kashevarov, et al., [The Crystal Ball at MAMI, TAPS, and A2 Collaborations], Eur. Phys. J. A 42 (2009) 141, DOI: 10.1140/epja/i2009-10868-4.
- [7] E. Gutz, V. Sokhoyan, H. van Pee, et al., [CBELSA/TAPS Collaboration], Eur. Phys. J. A 35 (2008) 291.
- [8] M. Doring, E. Oset, D Strottman, Phys. Rev. C 73 (2006) 045209.
- [9] A. Fix, V.L. Kashevarov, A. Lee, M. Ostrick, arXiv:1004.5240 [nucl-th].
- [10] A. Fix, M. Ostrick, L. Tiator, Eur. Phys. J. A 36 (2008) 61, DOI: 10.1140/epja/i2007-10551-x.
- [11] W. Roberts, T. Oed, Phys. Rev. C 71 (2005) 055201.

- [12] S. Strauch, et al., [CLAS Collaboration], Phys. Rev. Lett. 95 (2005) 162003.
- [13] D. Krambrich, et al., [Crystall Ball at MAMI, TAPS, and A2 Collaborations], Phys. Rev. Lett. 103 (2009) 052002, DOI: 10.1103/PhysRevLett.103.052002.
- [14] E. Gutz, V. Sokhoyan, H. van Pee, et al., [CBELSA/TAPS Collaboration], Phys. Lett. B 687 (2010) 11.
- [15] L. Roca, Nucl. Phys. A 748 (2005) 192.
- [16] M. Doring, E. Oset, U.-G. Meissner, arXiv:1003.0097 [nucl-th].
- [17] J.C. McGeorge, et al., Eur. Phys. J. A 37 (2008) 129.
- [18] K.-H. Kaiser, et al., Nucl. Instr. Meth. A 593 (2008) 159.
- [19] H. Olsen, L. C. Maximon, Phys. Rev. 114 (1959) 887.
- [20] A. Fix, H. Arenhövel, in preparation.